

# Improved Heat Transfer in Guar Gel Composites Reinforced with Randomly Distributed Glass Microspheres

Ruifeng CAO<sup>1</sup>, Taotao WANG<sup>1</sup>, Yuxuan ZHANG<sup>2</sup>, Hui WANG<sup>3\*</sup>

<sup>1</sup> School of Traffic Engineering, Huanghe Jiaotong University, Jiaozuo 454950, China

<sup>2</sup> School of Aerospace Engineering and Applied Mechanics, Tongji University, Shanghai 200082, China

<sup>3</sup> School of Civil Engineering and Architecture, Hainan University, Haikou 570228, China

**crossref** <http://dx.doi.org/10.5755/j02.ms.29824>

Received 16 September 2021; accepted 04 November 2021

Improved heat transfer in composites consisting of guar gel matrix and randomly distributed glass microspheres is extensively studied to predict the effective thermal conductivity of composites using the finite element method. In the study, the proper and probabilistic three-dimensional random distribution of microspheres in the continuous matrix is automatically generated by a simple and efficient random sequential adsorption algorithm which is developed by considering the correlation of three factors including particle size, number of particles, and particle volume fraction controlling the geometric configuration of random packing. Then the dependences of the effective thermal conductivity of composite materials on some important factors are investigated numerically, including the particle volume fraction, the particle spatial distribution, the number of particles, the nonuniformity of particle size, the particle dispersion morphology and the thermal conductivity contrast between particle and matrix. The related numerical results are compared with theoretical predictions and available experimental results to assess the validity of the numerical model. These results can provide good guidance for the design of advanced microsphere reinforced composite materials.

**Keywords:** composite, guar gel matrix, glass microsphere, thermal conductivity, randomness.

## 1. INTRODUCTION

Improved heat transfer in composites containing microspheres has received significant interest in the past decades for potential engineering applications which usually require higher or lower thermal conductivity than pure matrix material [1–4]. For example, to improve building energy efficiency, the spherically encapsulated phase change material can be embedded into cement material to form three-component composites [5–7]. Glass microspheres with hollow structure have been employed to increase the thermal insulation of composites with light weight [8–12]. Metal powders were added into a polymer matrix to fabricate composites with enhanced thermal conductivity and better mechanical properties [13, 14]. Besides, solid glass beads have been employed as filler to fabricate polymer composites without significant weight increase [15, 16]. More recently, it was demonstrated that the addition of glass beads to gel matrix can improve the thermal properties of the composites over a large range of filler volume fraction [17]. Thus, for the reason of thermal conduction assessment during structure design, it is necessary to understand how the particle influences the thermal property, especially thermal conductivity, of composites.

To predict the thermal conductivity of composite materials consisting of matrix and microspheres, some theoretical or empirical models, i.e. the series model [18], the parallel model [18], the Maxwell model [18, 19], and the Lewis-Nielsen model [20], have been developed and most of them are based on the regular distribution assumption of

microsphere in the matrix. However, it is difficult to keep the microspheres uniformly dispersed in the matrix in practical fabrication, as indicated in literature [8] and [21]. Thus, these theoretical models may not be suitable for randomly distributed microspheres. Moreover, the strong interaction between randomly dispersed microspheres greatly affects the thermal distribution in composites and then may influence the overall thermal conductivity of the composite. Such influences can't be fully characterized by the theoretical models. Therefore, the numerical prediction, mainly by finite element method, can be employed to provide a more flexible way for understanding complex heat transfer mechanisms in realistic random composites [22]. Currently, the major challenge is to establish a proper random composite model in which the random arrangement of microspheres is close to the real status, and then numerically and quantitatively predict the effective thermal conductivity of composite by considering several important microstructure factors including the thermal conductivity contrast of microsphere and matrix, the microsphere volume fraction, the number of microspheres, the microsphere size distribution and the microsphere dispersion morphology (degree of mixing).

This paper aims to study improved thermal transfer in composite consisting of guar gel matrix and solid glass microsphere by (1) developing a simple and efficient random sequential adsorption (RSA)-based algorithm to automatically generate a series of three-dimensional random arrangements of solid microspheres in the representative unit cell, with the predefined controlling geometric parameters including the microsphere volume fraction, the

\* Corresponding author. Tel.: +86-898-66279232; fax: +86-898-66279232. E-mail address: [huiwang@hainanu.edu.cn](mailto:huiwang@hainanu.edu.cn) (H. Wang)

number of microspheres and the microsphere size; (2) simulating thermal flow through the generated three-dimensional random composite model by finite element method; (3) rigorously analyzing the influence of several important factors to the thermal conductivity of random composite; and (4) assessing the validity of available theoretical predictions by comparing to numerical and experimental results. The results could guide for the application of solid glass microsphere filled guar gel-matrix composites.

## 2. GENERATION OF RANDOM DISTRIBUTION OF MICROSPHERES

The guar gel composites filled with glass microspheres that have been experimentally investigated in the first work by Charson [17] are taken as target materials in this study. Because the bulk physical properties of the composites have been revealed to be strongly dependent on their microstructures, the corresponding composite models need to be constructed critically on the level of microstructure. Particularly, the reconstruction of microstructure can be accomplished by the numerical algorithms [23–28] or the X-ray CT (computed tomography) scanning system [29], which usually involves complex digital image techniques and special device. In this study, three-dimensional random distribution of glass microspheres in a square domain is generated by the simple RSA algorithm [23] to produce a unit cell model mimicking the real morphology of microspheres in the matrix. The algorithm is programmed by following the three steps:

Step 1: the side length of the cubic unit cell is evaluated using of the following correlation of the microsphere volume fraction, the number of microspheres, the microsphere size and the cubic unit cell size as

$$v_p = \frac{n_p \times 4\pi r_p^3}{3a^3} \Rightarrow a = r_p \cdot \sqrt[3]{\frac{n_p \times 4\pi}{3v_p}}, \quad (1)$$

where  $v_p$  is the occupied volume fraction of microspheres,  $n_p$  denotes the number of microspheres with identical size,  $r_p$  represents the radius of the microsphere and  $a$  is the side length of the unit cell. Here, it is assumed that the microspheres have identical size for the sake of convenience.

Step 2: the location of each microsphere in the unit cell is randomly generated using a random number generator. It is assumed that (1) the microspheres don't overlap each other; (2) the microspheres don't intersect with the boundary faces of the unit cell. These restrictions simplify the evaluation of the microsphere volume fraction, and more importantly, they may be beneficial to create an adequate finite element mesh [10]. These control conditions can be represented by the following expressions (see Fig. 1):

$$[x_c, y_c, z_c] = \text{rand}(1,3) \times (a - 2r_p) + r_p; \quad (2)$$

$$d > d_{\min} = 2r_p, \quad (3)$$

where  $(x_c, y_c, z_c)$  are Cartesian coordinates of each microsphere center and the rand is a random number generator in the range of (0.1) in MATLAB.  $d$  and  $d_{\min}$

stand for the distance of central points of any two microspheres and their minimum value, respectively.

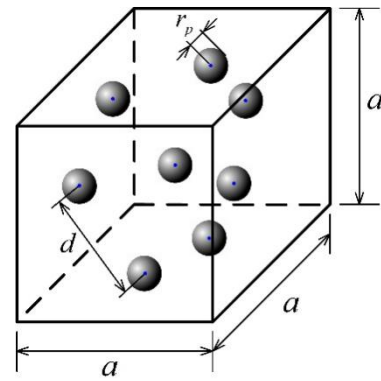


**Fig. 1.** Schematic diagram of the procedure of generating randomly dispersed microspheres in a cubic

Step 3: repeating Step 2 until no microsphere can be added into the unit cell.

To demonstrate this present algorithm, series random geometric models are generated in Fig. 2, in which the microsphere radius is uniformly taken as 1.75 mm, the number of microspheres is set to be 100, which is sufficiently high to make desired random composite models [30] and the microsphere volume fraction changes from 5 % to 30 %.

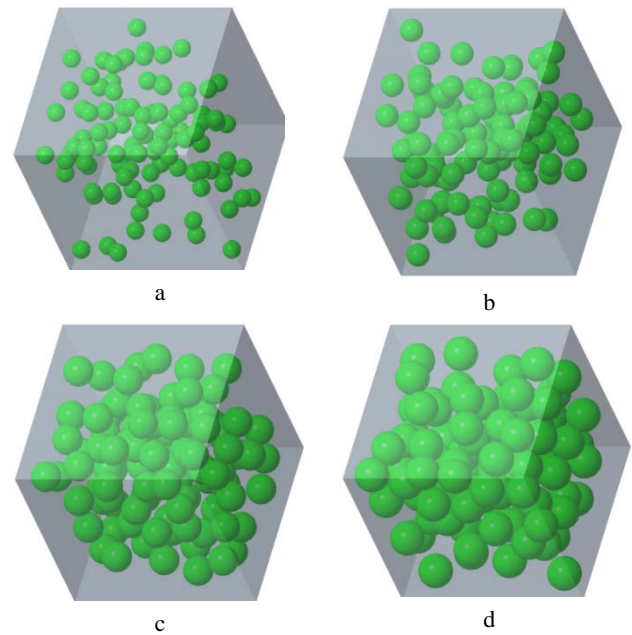


**Fig. 2.** Random arrangements of 100 spherical particles in the unit cell with various filler volume fractions: a –  $v_p = 5\%$ ; b –  $v_p = 10\%$ ; c –  $v_p = 20\%$ ; d –  $v_p = 30\%$

It is worth noting that the intersection check during the running of the algorithm will greatly increase computational time for increased filler volume fraction. Hence, the generated models are limited to filler volume fraction up to 30 %, which is a medium value for the 3D case. The corresponding Matlab code is given in the Appendix for reference. Additionally, the random models related to the different numbers of fillers are shown in Fig. 3 in which the filler volume fraction is assumed as 10 %. From Fig. 2 and Fig. 3, it can be indicated that the present algorithm is

efficient to produce random distributions of microspheres in the cubic unit cell by setting the filler size, the filler volume fraction, and the number of fillers.

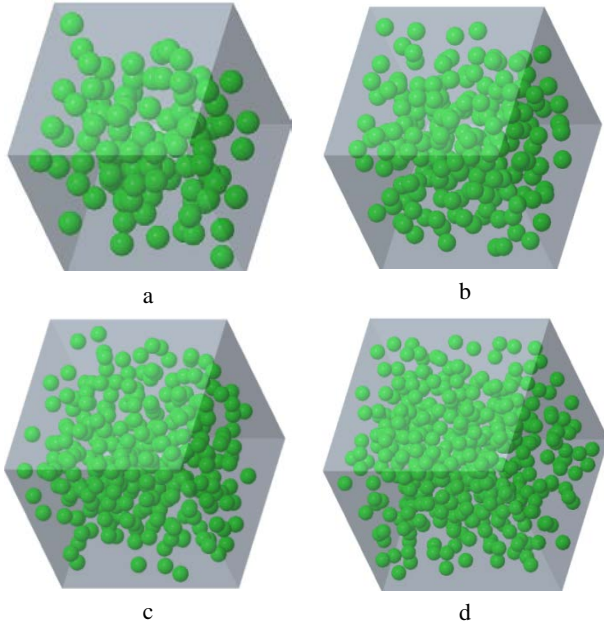


**Fig. 3.** Random arrangements of 10 % spherical particles in the unit cell with the different numbers of spheres: a- $n_p = 100$ ; b- $n_p = 200$ ; c- $n_p = 300$ ; d- $n_p = 400$

### 3. COMPUTATIONAL MODELING

In this study, we aim to investigate the effective thermal conductivity of microsphere reinforced composite materials represented by the generated random models. Fig. 4 displays a random model consisting of randomly dispersed microspheres and matrix. It is assumed that (1) all material components are isotropic and homogeneous; (2) there is no heat generation in the unit cell, and (3) the interfacial contact resistance between the microsphere and the matrix is neglected.

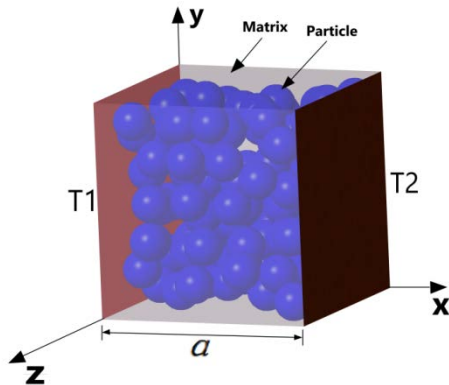


**Fig. 4.** Schematic diagram of transverse heat transfer in a unit cell containing randomly dispersed spherical particles

Under the above assumptions, the three-dimensional steady-state heat conduction in this two-phase composite model can be governed by the following partial differential equations [34]:

$$\nabla^2 T_p = 0, \quad \nabla^2 T_m = 0 \quad (4)$$

where  $T_p$  and  $T_m$  are local temperature in the spherical

particle and the matrix material.  $\nabla^2$  represents the Laplacian operator.

These governing equations have to be coupled with the specified boundary conditions to make the problem solvable. In Fig. 4, the different temperatures  $T_1$  and  $T_2$  are imposed respectively on the opposite faces of the unit cell located at  $x = 0$  and  $x = a$ , and other surfaces keep insulated, so that the heat conduction in the unit cell mainly takes place along the  $x$ -direction. Hence, the specified boundary conditions for the unit cell can be described as

$$T|_{x=0} = T_1, \quad T|_{x=a} = T_2, \quad (5)$$

$$q_y|_{y=0} = 0, \quad q_y|_{y=a} = 0, \quad q_z|_{z=0} = 0, \quad q_z|_{z=a} = 0, \quad (6)$$

where  $q_y$  and  $q_z$  denote the heat flux component along the  $y$ - and  $z$ -direction, respectively, and are given by Fourier's law:

$$q_y = -k_m \frac{\partial T_m}{\partial y}, \quad q_z = -k_m \frac{\partial T_m}{\partial z}. \quad (7)$$

Besides, the continuous conditions at the interface of microsphere and matrix can be written as

$$k_m \frac{\partial T_m}{\partial \mathbf{n}} = k_p \frac{\partial T_p}{\partial \mathbf{n}}, \quad T_m = T_p, \quad (8)$$

where  $\mathbf{n}$  is the unit normal vector to the matrix/sphere interface.

Solving the system described by Eq. 5, and Eq. 8 by the finite element simulation, the thermal flow and the temperature distribution in the unit cell can be obtained. Then, the effective thermal conductivity of composite material along the  $x$ -direction can be evaluated by

$$k_{eff} = -\frac{\tilde{q}_x a}{\Delta T}, \quad (9)$$

where  $\Delta T = T_2 - T_1$  is the temperature difference and the area-averaged heat flux

$$\tilde{q}_x = \frac{1}{A} \int_A q_x(x, y, z) dA. \quad (10)$$

with the real heat flux component  $q_x$  in the  $x$ -direction,  $A$  is the area of a selected cross-section perpendicular to the  $x$ -direction. Theoretically, any cross-section between  $x = 0$  and  $x = a$  can be chosen for evaluating  $\tilde{q}_x$ , here the right face  $x = a$  is typically chosen in the practical computation [4].

In this study, the glass beads with a diameter of 3.5  $\mu\text{m}$  were randomly dispersed in the guar gel matrix to form the two-phase composite material in literature [17], in which the matrix was made by mixing 4 % (mass basis) guar gel powder and 96 % water. The related material properties of filler and matrix are listed in Table 1.

**Table 1.** The related material properties of filler and matrix [17]

Material	Density, $\text{kg/m}^3$	Specific heat capacity, $\text{J/kg K}$	Thermal conductivity, $\text{W/m K}$
Glass bead	2520	800	1.1
Guar gel	1015	4150	0.57

## 4. THEORETICAL MODELS

Numerous theoretical models have been developed over the past decades for predicting the effective thermal conductivity of two-phase composite material consisting of spherical particle and matrix. In Table 2, some of these models are summarized for comparison. Based on the electric-thermal analog concept, the Series and Parallel models were derived by assuming that each material phase in the composite is arranged along the direction parallel or perpendicular to the heat flow direction and thus can give the lower and upper bounds of the effective thermal conductivity of the two-phase heterogeneous composite materials [18]. The Maxwell model assumed the distance between spherical inclusions was far larger than the sphere size, and then derived heat conduction through the medium in spherical coordinates under the given far-field temperature gradient [19]. The Lewis-Nielsen model was approximately given base on a vast amount of experimental data available on thermal conductivity of particle reinforced composites [20]. Undoubtedly, these theoretical models give effective thermal conductivity as a function of the particle volume fraction.

**Table 2.** Some theoretical models for microsphere reinforced composites

Model	Expression
Series [18]	$k_{eff} = \frac{k_m k_p}{k_m v_p + k_p v_m}$
Parallel [18]	$k_{eff} = k_p v_p + k_m (1 - v_p)$
Maxwell [19]	$k_{eff} = k_m \frac{2 + k_p / k_m - 2(1 - k_p / k_m)v_p}{2 + k_p / k_m + (1 - k_p / k_m)v_p}$
Lewis-Nielsen [20]	$k_{eff} = k_m \frac{1 + ABv_p}{1 - BCv_p}$ with $A = 1.5$ for rigid shpere $B = \frac{k_p / k_m - 1}{k_p / k_m + A}$ , $C = 1 + 1.323v_p$

## 5. RESULTS AND DISCUSSION

### 5.1. Mesh convergence

In the present work, the composite model established in the previous section is solved with linear tetrahedral finite element discretization. The mesh convergence is guaranteed by requiring that the relative difference in the predicted area-averaged heat flux  $\tilde{q}_x$  evaluated in Eq. 10 between two adjacent mesh densities characterized by the number of finite elements or nodes is less than 0.05 %.

During the convergence investigation, a unit cell containing 100 randomly distributed spherical particles is simulated with the imposed temperature conditions  $T_1=400$  K and  $T_2 = 300$  K, as indicated in Fig. 5. The filler volume fraction is assumed to be 30 %. Fig. 6 shows a typical mesh division of the matrix and the spherical particles using 403493 tetrahedral elements. Fig. 7 indicates the variation of the predicted local area-averaged heat flux

$\tilde{q}_x$  as the number of degrees of freedom (DOFs) of nodes increases.

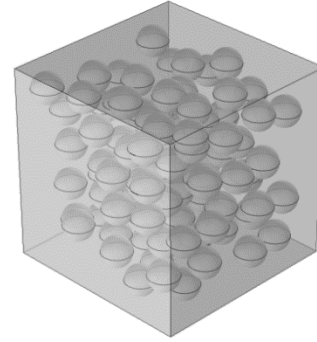


**Fig. 5.** Randomly dispersed spherical particles in the unit cell with 30 % filler volume fraction

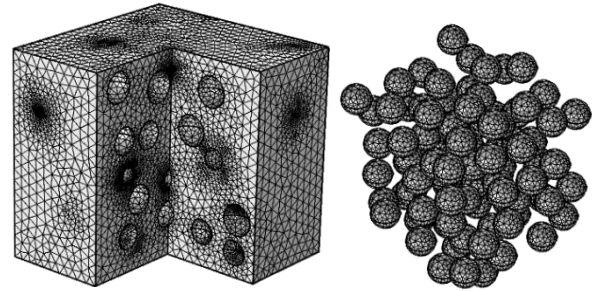


**Fig. 6.** Mesh configurations of the matrix (left) and the spherical particles (right)

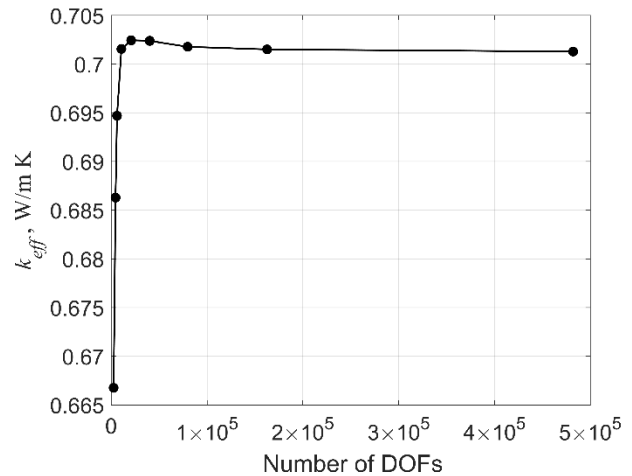


**Fig. 7.** Convergence investigation for different mesh densities

It is indicated from Fig. 7 that a converged result can be reached when the number of nodes increases to 80222. Besides, the distributions of temperature and heat flux component  $q_x$  on the mid-plane particular to the z-direction in the unit cell are plotted in Fig. 8. It is found from Fig. 8 a that the existence of a microsphere significantly changes the temperature distribution which becomes nonlinear in the unit cell domain. Moreover, the temperature gradient in the sphere and surrounding region is smaller than that in the matrix. For the heat flux shown in Fig. 8 b, in which the arrow represents the direction of heat flux and the thickness represents the intensity of heat flux, it can be seen that around the spherical particle, the thermal flow will converge and enhance. This can be attributed to the much higher thermal conductivity of glass beads than that of the Guar gel matrix. The thermal flow is usually collected to the particle

region with smaller heat resistance and can reach up to the maximum at the particle.

Especially, when the thermal conductivity of particle is set to be the same as that of the matrix, the linear heat conduction along the  $x$ -direction is expected under the specific boundary conditions, and the predicted area-averaged heat flux  $\tilde{q}_x$  is approximately equal to the exact solution  $k_m(T_1 - T_2)/a$ , as expected. Therefore, it can be concluded that the finite element model established for the random composite is validated.

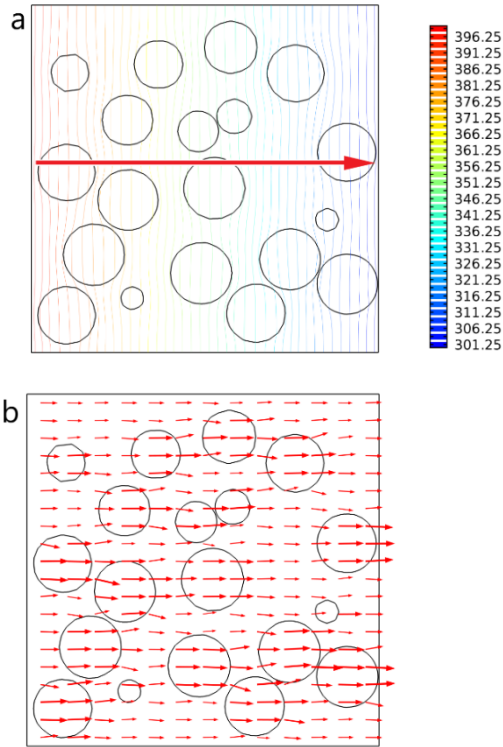


**Fig. 8.** a – temperature; b – heat flux distributions on the mid-plane particular to the  $x$ -direction of the unit cell

## 5.2. Effect of particle volume fraction

To examine the influence of particle volume fraction on the effective thermal conductivity of composite, thermal simulation is performed on a total of six composite unit cell models generated with the present random algorithm. The particle volume fraction is assumed to be ranged from 5 % to 30 %, and the number of particles is set to be 100. The sphere size keeps constant ( $r_p = 1.75$  mm). With  $k_m = 0.57$  W/m K and  $k_p = 1.1$  W/m K, Fig. 9 shows the effective thermal conductivity  $k_{eff}$  of composites with randomly packed microspheres, and it is indicated that  $k_{eff}$  is strongly dependent on the particle volume fraction and increases with the increase of  $v_p$  nonlinearly. Additionally, the predicted results from the theoretical models and the experiment [17] are also provided in Fig. 9 for comparison. The error bars in Fig. 9 are based on the estimated uncertainty in the effective thermal conductivity data of  $\pm 5\%$ . It is observed from Fig. 9 that the theoretical predictions from the series and parallel models form the lower and upper limits to the effective thermal conductivity, and the numerical results and other theoretical predictions from the Lewis-Nielsen model and the Maxwell model

locate between them. Besides, the numerical results display similar behavior to the Maxwell model in the specific range of particle volume fraction. More importantly, it is observed that the numerical and theoretical results are all overestimated to the experiment results, but the predictions from the series model fit the experimental results better than others. The main reason is that the contact among spheres is neglected for both the numerical prediction and the other theoretical predictions. The particles in practice can touch and form thermal conductive chains. A similar conclusion was also obtained by Qiao et.al. [21].

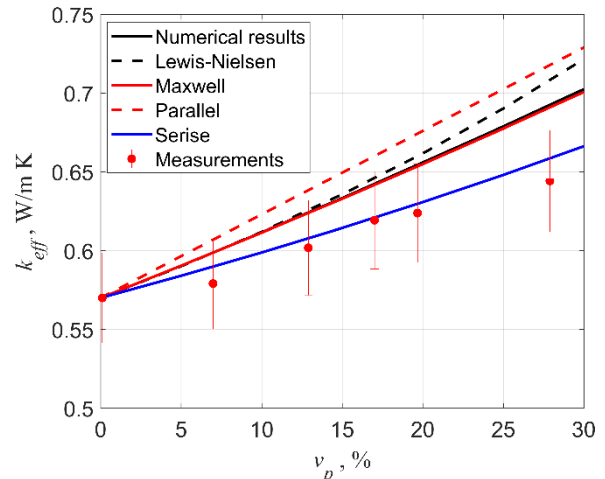


**Fig. 9.** Effective thermal conductivity of composite as a function of the particle volume fraction

## 5.3. Effect of random packing arrangement

Due to the real randomness of each particle position, each run of the present algorithm may generate a different packing arrangement of particles, even if the controlling parameters  $v_p$ ,  $n_p$  and  $r_p$  keep unchanged. Thus, it is necessary to investigate the effect of dispersion of spheres on the effective thermal conductivity  $k_m$ . For this aim, two different arrangements are generated for each value of  $v_p$  based on the same conditions  $n_p = 100$ ,  $r = 1.35$  mm. For example, Fig. 10 shows the two random configurations for the case of  $v_p = 30\%$ .

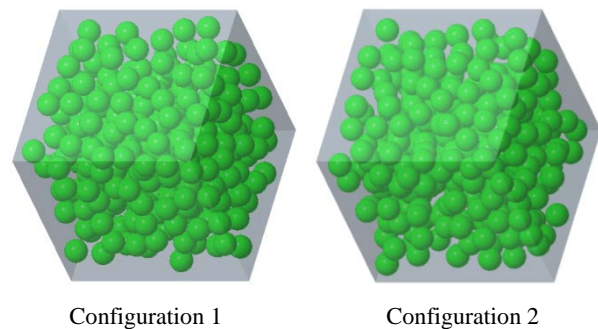


**Fig. 10.** Two different particle arrangements generated under the same predefined parameters

Using the finite element analysis, the effective thermal conductivity  $k_m$  of composites can be evaluated, as tabulated in gray in Table 3. It is found that the two different random packing arrangements give almost same results. Therefore, it can be concluded that the effective thermal

conductivity of composite is almost independent of the variation of random particle arrangement. A similar conclusion was drawn for the three-component composites consisting of matrix, PCM core and solid shell in literature [5].

**Table 3.** Effective thermal conductivity (W/m K) of composites for different random particle arrangements

$v_p$	Configuration 1	Configuration 2
5 %	0.5910	0.5879
10 %	0.6117	0.6118
15 %	0.6340	0.6333
20 %	0.6561	0.6563
25 %	0.6794	0.6787
30 %	0.7018	0.7030

#### 5.4. Effect of the number of particles

Under the given sphere volume fraction and sphere size, the size of the unit cell is only related to the number of spheres inside it. To illustrate this, we limit the spherical radius to be 1.75 mm and permit the filler volume fraction to change from 5 % to 30 %. The resulted effective thermal conductivity shown in gray is given in Table 4, from which it is indicated that the number of spheres in the unit cell has a slight effect on the composite thermal conductivity.

**Table 4.** Effective thermal conductivity (W/m K) of composites for various numbers of spheres

$\frac{n_p}{v_p}$	55	65	75	100	200	300
5%	0.5910	0.5909	0.5909	0.5910	0.5906	0.5908
10%	0.6120	0.6117	0.6119	0.6117	0.6119	0.6119
15%	0.6337	0.6336	0.6334	0.6340	0.6338	0.6336
20%	0.6556	0.6553	0.6562	0.6561	0.6564	0.6560
25%	0.6792	0.6785	0.6798	0.6794	0.6782	0.6794
30%	0.7023	0.7010	0.7027	0.7018	0.7026	0.7024

#### 5.5. Effect of particle size

The realistic particle size is non-uniform [5, 16, 17, 31]. Thus, considering the effect of nonuniform particle size is necessary to incorporate the actual particle size distribution. To do this, Eq. 1 should be revised as

$$v_p = \frac{4\pi}{3a^3} \times \sum_{i=1}^m (n_p^i \times r_p^{i3}), \quad (11)$$

where  $n_p^i$  is the number of particles with a radius  $r_p^i$ , and  $m$  is the total number of size distributions. Here, for the sake of convenience, only two particle sizes are considered, i.e.  $r_p^1 = 1.75$  mm and  $r_p^2 = 5$  mm, and each size corresponds to 50 spherical particles. If the particle volume fraction is 30%, the side length of the unit cell is evaluated from Eq. 11 as 44.9807 mm. Fig. 11 shows the generated computational composite model containing the two types of particles size. Compared to the numerical prediction (0.7018 W/m K in Table 4) of 100 particles with a uniform radius of 1.75 mm, the effective thermal conductivity  $k_{eff}$  of such composite containing differently sized particles is 0.7020 W/m K. Thus, the effect of nonuniformity of particle size can be ignored in practice.

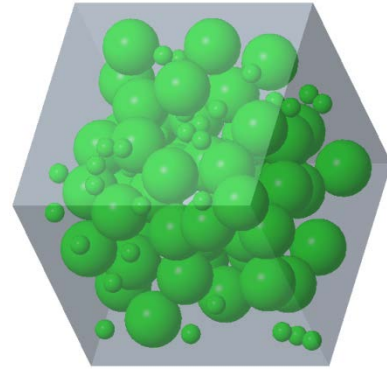


**Fig. 11.** Unit cell containing two types of particle size

#### 5.6. Effect of constituent thermal conductivity contrast

Fig. 12 plots the effective thermal conductivity  $k_{eff}$  of a composite material containing 100 randomly dispersed spheres as a function of sphere thermal conductivity  $k_p$  ranging from 0.001 to 0.5 W/m K for 30 % filler volume fraction. The thermal conductivity  $k_m$  of matrix keeps 0.57 W/m K unchanged. The particle size is  $r_p = 1.75$  mm. The results in Fig. 12 clearly demonstrate that the numerical predictions of  $k_{eff}/k_m$  is a nonlinear function of the material ratio  $k_p/k_m$ . Such nonlinearity can be explained by the analytical Maxwell model, which is rewritten as

$$\frac{k_{eff}}{k_m} = \frac{2 - 2v_p + (1 + 2v_p)k_p / k_m}{2 + v_p + (1 - v_p)k_p / k_m} \quad (12)$$

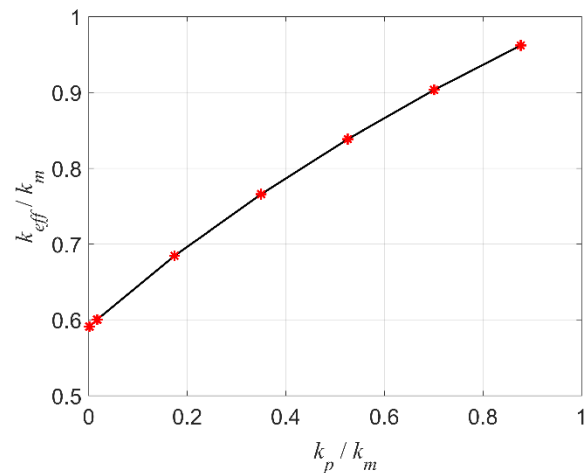


**Fig. 12.** Effective thermal conductivity of composites for various values of thermal conductivity contrast

## 6. CONCLUSIONS

In this study, the three-dimensional random model of randomly-dispersed glass microsphere reinforced guar gel matrix composite is developed by the present random algorithm and then a comprehensive study on the influences of some controlling parameters on the improved effective thermal conductivity of composites is carried out by finite element simulation. The numerical results show that:

1. the present RSA-based algorithm is simple and efficient to produce random distribution of particles in a unit cell with specific filler volume content up to 30% or higher;

- the improved thermal conductivity of composites strongly depends on the filler volume fraction and the thermal conductivity contrast between particle and matrix, rather than the particle numbers, the particle random packing arrangement and the dispersion of particle size;
- the present computational predictions are very close to the Maxwell model and both of them are always higher than the experimental results;
- The series model fit the experimental results better than others.

### Acknowledgments

The research was financially supported by the National Natural Science Foundation of China (No. 12072107) and Henan Province University Innovation Group Support Program (No. 19IRTSTHN020).

### Appendix 1. Matlab code for generating random distribution of spheres in the cubic unit cell

```
function Coord=SphereCenter(vp, rp, np)
%The generation of random spheres in a cubic
% vp: particle volume fraction
% rp: radius of each particle
% np: number of particles
s=((4/3)*pi*np)/(vp)^(1/3)*rp; % Side length of
unit cell
Coord1=rand(1,3)*(s-2*rp)+rp; % First random
coordinates
dmin=2*rp;
m=1; % Counter
while m<np
    Coord=rand(1,3)*(s-2*rp)+rp; % Produce new
coordinates
    dist=sqrt(sum((Coord-Coord1).^2,2)); %
Distance
    if dist>dmin
        m=m+1;
        Coord1=[Coord1;Coord];
    end
end
% Output data
fp=fopen('SphereCenter.txt','wt');
for ip=1:np
    xp=Coord1(ip,1);
    yp=Coord1(ip,2);
    zp=Coord1(ip,3);
    fprintf(fp,'%10.8e, %10.8e,
%10.8e\n',xp,yp,zp);
end
fclose(fp);
```

### REFERENCES

- Lee, J.K.** Prediction of Thermal Conductivity of Composites with Spherical Fillers by Successive Embedding *Archive of Applied Mechanics* 77 (7) 2007: pp. 453–460. <https://doi.org/10.1007/s00419-006-0108-7>
- Pal, R.** Thermal Conductivity of Three-Component Composites of Core-Shell Particles *Materials Science and Engineering: A* 498 (1–2) 2008: pp. 135–141. <https://doi.org/10.1016/j.msea.2007.10.123>
- Ngo, I.L., Byon, C.** A Generalized Correlation for Predicting the Thermal Conductivity of Composite Materials *International Journal of Heat and Mass Transfer* 83 2015: pp. 408–415. <https://doi.org/10.1016/j.ijheatmasstransfer.2014.11.088>
- Kumlutas, D., Tavman, I.H.** A Numerical and Experimental Study on Thermal Conductivity of Particle Filled Polymer Composites *Journal of Thermoplastic Composite Materials* 19 (4) 2016: pp. 441–455. <https://doi.org/10.1177/0892705706062203>
- Thiele, A.M., Kumar, A., Sant, G., Pilon, L.** Effective Thermal Conductivity of Three-Component Composites Containing Spherical Capsules *International Journal of Heat and Mass Transfer* 73 2014: pp. 177–185. <https://doi.org/10.1016/j.ijheatmasstransfer.2014.02.002>
- Ngo, I.L., Byon, C.** An Extensive Study on Enhancing the Thermal Conductivity of Core-Shell Nanoparticle Composites Using Finite Element Method *International Journal of Heat and Mass Transfer* 101 2016: pp. 147–155. <https://doi.org/10.1016/j.ijheatmasstransfer.2016.05.046>
- Ricklefs, A., Thiele, A.M., Falzone, G., Sant, G., Pilon, L.** Thermal Conductivity of Cementitious Composites Containing Microencapsulated Phase Change Materials *International Journal of Heat and Mass Transfer* 104 2017: pp. 71–82. <https://doi.org/10.1016/j.ijheatmasstransfer.2016.08.013>
- Yung, K., Zhu, B., Yue, T., Xie, C.** Preparation and Properties of Hollow Glass Microsphere-Filled Epoxy-Matrix Composites *Composites Science and Technology* 69 (2) 2009: pp. 260–264. <https://doi.org/10.1016/j.compscitech.2008.10.014>
- Patankar, S.N., Kranov, Y.A.** Hollow Glass Microsphere HDPE Composites for Low Energy Sustainability *Materials Science and Engineering: A* 527 (6) 2010: pp. 1361–1366. <https://doi.org/10.1016/j.msea.2009.10.019>
- Yu, M., Zhu, P., Ma, Y.** Effects of Particle Clustering on The Tensile Properties and Failure Mechanisms of Hollow Spheres Filled Syntactic Foams: A Numerical Investigation by Microstructure Based Modeling *Materials & Design* 47 2013: pp. 80–89. <https://doi.org/10.1016/j.matdes.2012.12.004>
- Ren, S., Liu, J., Guo, A., Zang, W., Geng, H., Tao, X., Du, H.** Mechanical Properties and Thermal Conductivity of a Temperature Resistance Hollow Glass Microspheres/Borosilicate Glass Buoyance Material *Materials Science and Engineering: A* 674 2016: pp. 604–614. <https://doi.org/10.1016/j.msea.2016.08.014>
- Liu, B., Wang, H., Qin, Q.H.** Modelling and Characterization of Effective Thermal Conductivity of Single Hollow Glass Microsphere and Its Powder *Materials (Basel)* 11 (1) 2018: pp. 133. <https://doi.org/10.3390/ma11010133>
- Tekce, H.S., Kumlutas, D., Tavman, I.H.** Effect of Particle Shape on Thermal Conductivity of Copper Reinforced Polymer Composites *Journal of Reinforced Plastics and Composites* 26 (1) 2016: pp. 113–121. <https://doi.org/10.1177/0731684407072522>
- Joo, S.J., Hwang, H.J., Kim, H.S.** Highly Conductive Copper Nano/Microparticles Ink via Flash Light Sintering for Printed Electronics *Nanotechnology* 25 (26) 2014: pp. 265601. <https://doi.org/10.1088/0957-4484/25/26/265601>
- Yang, W., Liu, Z.Y., Shan, G.F., Li, Z.M., Xie, B.H., Yang, M.B.** Study on the Melt Flow Behavior of Glass Bead Filled Polypropylene *Polymer Testing* 24 (4) 2005: pp. 490–497. <https://doi.org/10.1016/j.polymertesting.2004.12.005>
- Lepez, O., Choplin, L., Tanguy, P.A.** Thermorheological Analysis of Glass Beads-Filled Polymer Melts *Polymer*

- Engineering & Science* 30 (14) 1990: pp. 821–828.  
<https://doi.org/10.1002/pen.760301404>
17. **Carson, J.K.** Thermal Diffusivity and Thermal Conductivity of Dispersed Glass Sphere Composites Over a Range of Volume Fractions *International Journal of Thermophysics* 39 (6) 2018: pp. 70.  
<https://doi.org/10.1007/s10765-018-2392-1>
  18. **Carson, J.K., Lovatt, S.J., Tanner, D.J., Cleland, A.C.** Thermal Conductivity Bounds for Isotropic, Porous Materials *International Journal of Heat and Mass Transfer* 48 (11) 2005: pp. 2150–2158.  
<https://doi.org/10.1016/j.ijheatmasstransfer.2004.12.032>
  19. **Maxwell, J.** A Treatise on Electricity and Magnetism *Nature* 7 (182) 1873: pp. 478–480.  
<https://doi.org/10.1038/007478a0>
  20. **Lewis, T.B., Nielsen, L.E.** Dynamic Mechanical Properties of Particulate-Filled Composites *Journal of Applied Polymer Science* 14 (6) 1970: pp. 1449–1471.  
<https://doi.org/10.1002/app.1970.070140604>
  21. **Qiao, Y., Wang, X., Zhang, X., Xing, Z.** Thermal Conductivity and Compressive Properties of Hollow Glass Microsphere Filled Epoxy–Matrix Composites *Journal of Reinforced Plastics and Composites* 34 (17) 2015: pp. 1413–1421.  
<https://doi.org/10.1177/0731684415592172>
  22. **Qian, L., Pang, X., Zhou, J., Yang, J., Lin, S., Hui, D.** Theoretical Model and Finite Element Simulation on the Effective Thermal Conductivity of Particulate Composite Materials *Composites Part B: Engineering* 116 2017: pp. 291–297.  
<https://doi.org/10.1016/j.compositesb.2016.10.067>
  23. **Widom, B.** Random Sequential Addition of Hard Spheres to a Volume *The Journal of Chemical Physics* 44 (10) 1966: pp. 3888–3894.  
<https://doi.org/10.1063/1.1726548>
  24. **Wang, H., Zhao, X.J., Wang, J.S.** Interaction Analysis of Multiple Coated Fibers in Cement Composites by Special N-Sided Interphase/Fiber Elements *Composites Science and Technology* 118 2015: pp. 117–126.  
<https://doi.org/10.1016/j.compscitech.2015.08.022>
  25. **Wang, H., Qin, Q.H., Xiao, Y.** Special n-sided Voronoi Fiber/matrix Elements for Clustering Thermal Effect in Natural-Hemp-Fiber-Filled Cement Composites *International Journal of Heat and Mass Transfer* 92 2016: pp. 228–235.  
<https://doi.org/10.1016/j.ijheatmasstransfer.2015.08.093>
  26. **Li, G., Sharifpour, F., Bahmani, A., Montesano, J.** A New Approach to Rapidly Generate Random Periodic Representative Volume Elements for Microstructural Assessment of High Volume Fraction Composites *Materials & Design* 150 2018: pp. 124–138.  
<https://doi.org/10.1016/j.matdes.2018.04.031>
  27. **Lin, W.Q., Zhang, Y.X., Wang, H.** Thermal Conductivity of Unidirectional Composites Consisting of Randomly Dispersed Glass Fibers and Temperature-Dependent Polyethylene Matrix *Science and Engineering of Composite Materials* 26 (1) 2019: pp. 412–422.  
<https://doi.org/10.1515/secm-2019-0024>
  28. **Weng, L., Fan, T., Wen, M., Shen, Y.** Three-Dimensional Multi-Particle FE Model and Effects of Interface Damage, Particle Size and Morphology on Tensile Behavior of Particle Reinforced Composites *Composite Structures* 209 2019: pp. 590–605.  
<https://doi.org/10.1016/j.compstruct.2018.11.008>
  29. **Garcea, S.C., Wang, Y., Withers, P.J.** X-ray Computed Tomography of Polymer Composites *Composites Science and Technology* 156 2018: pp. 305–319.  
<https://doi.org/10.1016/j.compscitech.2017.10.023>
  30. **Gluzman, S., Mityushev, V., Nawalaniec, W.** Computational Analysis of Structured Media. Academic Press, 2018.
  31. **Ren, S., Li, X., Zhang, X., Xu, X., Dong, X., Liu, J., Du, H., Guo, A.** Mechanical Properties and High-Temperature Resistance of the Hollow Glass Microspheres/Borosilicate Glass Composite with Different Particle Size *Journal of Alloys and Compounds* 722 2017: pp. 321–329.  
<https://doi.org/10.1016/j.jallcom.2017.06.092>



© Cao et al. 2022 Open Access This article is distributed under the terms of the Creative Commons Attribution 4.0 International License (<http://creativecommons.org/licenses/by/4.0/>), which permits unrestricted use, distribution, and reproduction in any medium, provided you give appropriate credit to the original author(s) and the source, provide a link to the Creative Commons license, and indicate if changes were made.